ACS APPLIED MATERIALS & INTERFACES

Research Article

www.acsami.org

Preparation of Highly Dispersed Reduced Graphene Oxide Decorated with Chitosan Oligosaccharide as Electrode Material for Enhancing the Direct Electron Transfer of *Escherichia coli*

Zhimin Luo,[†] Dongliang Yang,[†] Guangqin Qi,[†] Lihui Yuwen,[†] Yuqian Zhang,[†] Lixing Weng,*[,§] Lianhui Wang,*[,†] and Wei Huang*[,†,‡]

[†]Key Laboratory for Organic Electronics & Information Displays and Institute of Advanced Materials (IAM), Jiangsu National Synergetic Innovation Center for Advanced Materials (SICAM), Nanjing University of Posts and Telecommunications, 9 Wenyuan Road, Nanjing 210023, P. R. China

[‡]Key Laboratory of Flexible Electronics (KLOFE) & Institute of Advanced Materials (IAM), Jiangsu National Synergetic Innovation Center for Advanced Materials (SICAM), Nanjing Tech University (NanjingTech), 30 South Puzhu Road, Nanjing 211816, P. R. China

[§]College of Geography and Biological Information, Nanjing University of Posts and Telecommunications, 9 Wenyuan Road, Nanjing 210046, P. R. China

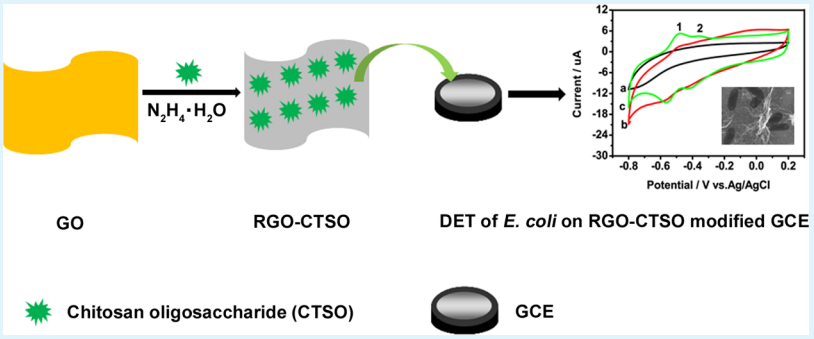

ABSTRACT: Water-dispersed reduced graphene oxide/chitosan oligosaccharide (RGO-CTSO) was prepared by chemical reduction of graphene oxide and synchronous functionalization with biocompatible chitosan oligosaccharide (CTSO). ζ potential measurement indicated that RGO-CTSO was highly stable in the acidic aqueous solution. RGO-CTSO was used to modify glassy carbon electrode (GCE) as the growth template of *Escherichia coli* (*E. coli*). The enhanced direct electron transfer of *E. coli* on the RGO-CTSO-modified GCE was studied by cyclic voltammetry. Compared with GCE or RGO-modified GCE, RGO-CTSO-modified GCE was more suitable for the adhesion growth of *E. coli* to improve direct electron transfer. The biocompatibility and versatility of RGO-CTSO made it promising for use as an anode material in microbial fuel cells.

KEYWORDS: *reduced graphene oxide, chitosan oligosaccharide, Escherichia coli, direct electron transfer*

1. INTRODUCTION

Environmental pollution is becoming a more serious problem caused by the overconsumption of energy based on petroleum and coal. Microbial fuel cells (MFCs), as a new technology for developing a clean energy source, have recently attracted a great deal of attention. However, their development is limited by sluggish electron transfer between the anode and microorganism, which leads to their low energy conversion and power.[1−4] Great efforts have been made to promote electron transfer between the anode and bacteria.[1] For example, mediators have been used to modify electrodes to enhance electron transfer in *Escherichia coli*.[5] However, the effect of the mediator relies on its redox potential, which needs to be lower than the anode potential and higher than the potential of the bacterial outer membrane.[5,6] In addition, the electrodes functionalized with a mediator are often unstable.[5,6] Electrodes decorated with nanomaterials may be an efficient avenue for significantly improving the output power density of MFCs. The nanomaterials used as the anode of MFCs are required to fit for adhesion growth of bacteria and have the ability to promote their direct electron transfer (DET).

Graphene, a new kind of two-dimensional sp^2-hybridized carbon nanomaterial, has various applications: supercapacitors, lithium batteries, biosensors, fuel cells, etc.[7−9] Graphene had been studied as a kind of anode material for enhancing DET of the bacterium *Pseudomonas aeruginosa*.[1] Nonetheless, the DET of *E. coli* on electrodes modified with graphene or a graphene nanocomposite has not been reported to the best of our

Received: January 11, 2015
Accepted: April 8, 2015
Published: April 20, 2015

DOI: 10.1021/acsami.5b00297
ACS Appl. Mater. Interfaces 2015, 7, 8539−8544

Scheme 1. Preparation of RGO-CTSO

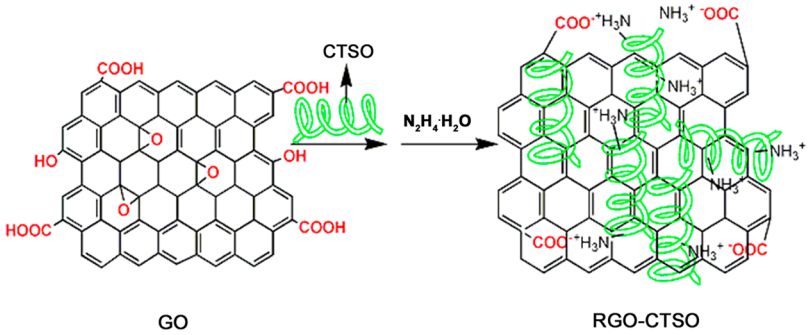

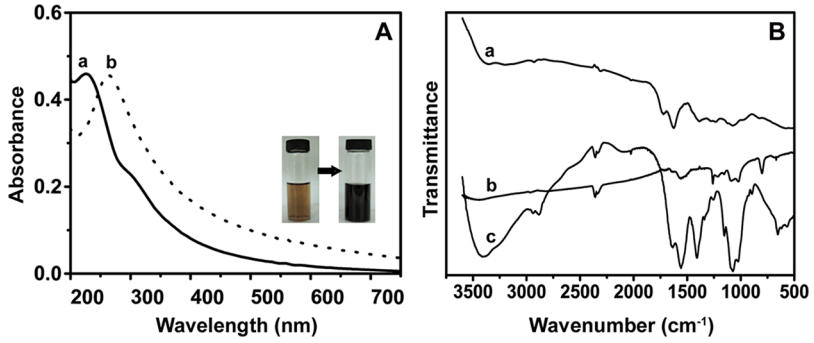

Figure 1. (A) UV−vis spectra of (a) GO and (b) RGO-CTSO. (B) FTIR spectra of (a) GO, (b) CTSO, and (c) RGO-CTSO.

knowledge. The readily available *E. coli* strain has been well explicated as a direct mediatorless biocatalyst in MFCs, but the electronegativity of graphene encumbers the adhesion growth of *E. coli* on the surface of an electrode modified with graphene and thus restrains the DET of *E. coli*.[10] Chitosan, a natural cationic polysaccharide derived from chitin, has been widely applied as an antimicrobial agents, a drug carrier, and an electrode material because of its biocompatibility, biodegradability, hydrophilicity, and excellent film forming property.[11,12] Modification of nanomaterials with chitosan can alter their surface properties for different applications. For example, a carbon nanotube could be rendered highly water-dispersed, electropositive, and biocompatible through noncovalent modification with chitosan as a cationic surfactant.[13]

Herein, reduced graphene oxide/chitosan oligosaccharide nanocomposites (RGO-CTSO) were prepared via chemical reduction of graphene oxide (GO) with water-soluble CTSO as a stabilizer. The adhesion growth as well as the DET of *E. coli* on the RGO-CTSO-modified glassy carbon electrode (GCE) was investigated. The significant enhancement of DET in *E. coli* resulted from *E. coli* adhesion and growth on RGO-CTSO-modified GCE, which shed light on a convenient and effective method for anode modification in MFCs.

2. EXPERIMENTAL SECTION

2.1. Materials. Hydrazine hydrate (50%), graphite, and CTSO (M_w = 1500) were purchased from Sigma-Aldrich. All chemicals used in the experiments were of analytical grade.

2.2. Synthesis of RGO-CTSO and RGO. A GO aqueous suspension was first synthesized by the previously reported method;[14−16] 2 mL of GO (2 mg mL^{-1}), 16 mL of deionized water, and 2 mL of CTSO (1 mg mL^{-1}) were mixed together and ultrasonicated for 2 h. Then the solution containing GO and CTSO was heated to 90 °C and held for 90 min after the addition of 5.6 μL of hydrazine hydrate (50 wt %). The final product was obtained through dialysis of the prepared suspension in deionized water for 3 days. RGO was synthesized by reducing GO directly with hydrazine hydrate without CTSO.

2.3. Preparation of Modified Electrodes. RGO-CTSO was dispersed in an acidic solution to form the RGO-CTSO suspension. Three microliters of the RGO-CTSO or RGO suspension (0.1 mg mL^{-1}) was dropped twice on the polished and cleaned GCE (3 mm diameter) and dried in the air at room temperature.

2.4. Study of DET between an Electrode and *E. coli*. GCE and GCE modified with RGO or RGO-CTSO were immersed in 5 mL of Luria Broth (LB) liquid culture medium containing *E. coli* and incubated under aerobic conditions at 35 °C for 12 h. Then each electrode was carefully washed with deionized water and immersed in a 0.1 M phosphate-buffered saline solution [PBS (pH 7.0)] for measuring DET in *E. coli* through cyclic voltammetry (CV).

2.5. Characterization. UV−vis and FTIR spectra of RGO-CTSO and GO were recorded on a UV−vis−NIR spectrophotometer (Shimadzu UV-3150) and FTIR spectrophotometer (Shimadzu IRPrestige-21), respectively. A scanning probe microscope (Shimadzu, model SPM-9500J3) and high-resolution transmission electron microscope (HRTEM) (JEOL, JEM-2010F UHR) were utilized for morphological characterization. Aqueous suspensions of RGO-CTSO and GO were dropped onto a carbon microgrid and dried for HRTEM characterization. Tapping mode with a height profile was adopted for AFM characterization after samples had been dropped onto a mica substrate. Raman spectra of RGO-CTSO, GO, and graphite were recorded with a Raman microspectrometer (Renishaw INVIA Reflex) with a 514 nm diode laser for excitation.

3. RESULTS AND DISCUSSION

CTSO is a linear polysaccharide composed of randomly distributed β-(1−4)-linked D-glucosamine and *N*-acetyl-D-glucosamine. Plentiful active amino groups of CTSO can interact with functional groups on the GO nanosheets.[18−24] Therefore, when GO was mixed with CTSO under acidic or neutral conditions, CTSO could be self-assembled on GO through hydrogen bonding and electrostatic interaction.[25] After GO was reduced by hydrazine hydrate in the presence of

DOI: 10.1021/acsami.5b00297
ACS Appl. Mater. Interfaces 2015, 7, 8539−8544

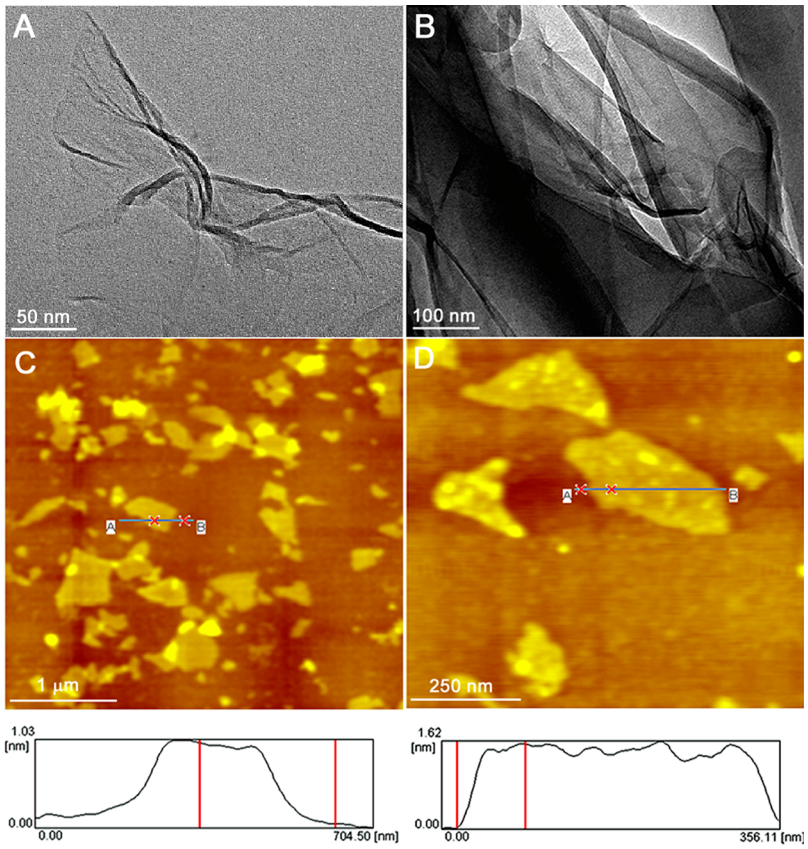

Figure 2. HRTEM images of (A) corrugated GO and (B) RGO-CTSO nanosheets. AFM images of (C) GO and (D) RGO-CTSO.

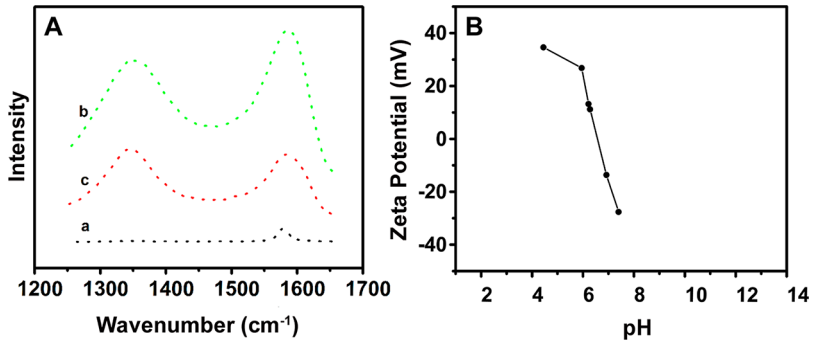

Figure 3. (A) Raman spectra of (a) graphite, (b) GO, and (c) RGO-CTSO. (B) ζ potential of RGO-CTSO in an aqueous solution at different pH values.

CTSO, the resultant RGO-CTSO remained stable in the acidic aqueous solution with CTSO on the surface as a cationic surfactant. The preparation of RGO-CTSO is shown in Scheme 1.

Chemical reduction of GO with CTSO as a stabilizer was measured by UV−vis spectroscopy (Figure 1A). The brown colloidal suspension of GO became black after it was reduced by hydrazine hydrate in the presence of CTSO. The UV−vis spectrum of the GO aqueous solution displayed two characteristic absorption peaks at 227 and 301 nm, which are assigned to $\pi \rightarrow \pi^*$ transitions of aromatic C−C bonds and $n \rightarrow \pi^*$ transitions of the carbonyl bond, respectively.[15,17,26] After reduction, the characteristic peak at 227 nm red-shifted to 264 nm and the peak at 301 nm was no longer present, suggesting the reduction of GO by hydrazine hydrate and restoration of electronic conjugation within RGO.[23,24,27] The functionalization of RGO by CTSO was validated by FTIR (Figure 1B). After GO was reduced by hydrazine hydrate in the presence of CTSO, the C═O vibration band (1722 cm^{-1}) of carboxyl became weaker and O−H bond deformation of the C−OH groups on GO (1384 cm^{-1}) was absent. The C−O stretch vibration of epoxy groups on GO at 1223 cm^{-1} also disappeared. The amide I band (1647 cm^{-1}) and the amide II band (1557 cm^{-1}) of CTSO in the FTIR spectrum of RGO-CTSO (c) appeared. FTIR characterization indicated that GO was reduced by hydrazine hydrate and simultaneously modified with CTSO successfully.[12,18,28,29]

The morphologies of GO and RGO-CTSO were characterized by HRTEM and AFM. As shown from the HRTEM images of GO (Figure 2A) and RGO-CTSO (Figure 2B), a transparent GO sheet with some corrugations supported on the carbon microgrid was clearly observed and the gauzy single-

DOI: 10.1021/acsami.5b00297
ACS Appl. Mater. Interfaces 2015, 7, 8539−8544

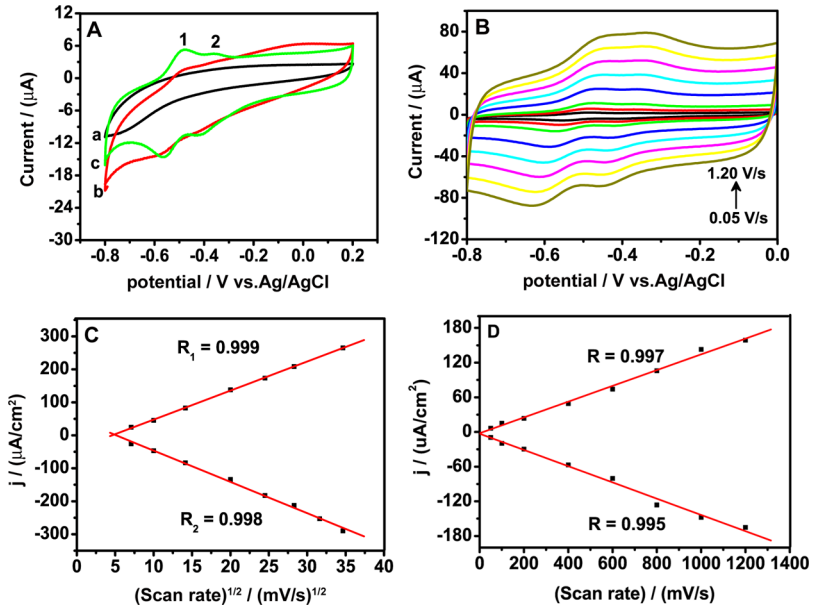

Figure 4. (A) CV of (a) GCE, (b) RGO-modified GCE, and (c) RGO-CTSO-modified GCE immersed in 5 mL of LB liquid culture medium containing *E. coli* and incubated at 35 °C under aerobic conditions for 12 h at a scan rate of 100 mV s^{-1}. (B) CV of RGO-CTSO-modified GCE immersed in 5 mL of LB liquid culture medium containing *E. coli* and incubated at 35 °C under aerobic conditions for 12 h at different scan rates from 0.05 to 1.20 V s^{-1}. (C) Linear curves of the peak current (peak 1) vs the square root of the scan rate. (D) Linear curves of the peak current (peak 2) vs the scan rate.

layer RGO-CTSO nanosheet was suspended and scrolled. The average thickness of GO sheets was determined to be ~0.95 nm by AFM characterization (Figure 2C), which confirmed the formation of single-layer GO.[30] The lateral dimension of GO was approximately 100−500 nm. From the AFM image of RGO-CTSO (Figure 2D), the thickness of RGO-CTSO was approximately 1.55 nm (>0.95 nm), which can be ascribed to the coverage of CTSO on the RGO nanosheet.

Raman characterization of GO and RGO-CTSO further demonstrated the structural evolution of GO after chemical reduction in the presence of CTSO. The typical features of Raman spectra are a G band at 1580 cm^{-1} assigned to the E_{2g} phonon of C sp^2 atoms and a D band at 1345 cm^{-1} assigned to a breathing mode of κ-point phonons of A_{1g} symmetry.[15−17,30] From the Raman spectrum of graphite in Figure 3A, a weak D band at 1345.3 cm^{-1} and an intensive G band at 1578.6 cm^{-1} were observed. The G bands in Raman spectra of GO and RGO-CTSO were broadened and shifted upward to 1584.6 cm^{-1} (GO) and 1581.9 cm^{-1} (RGO-CTSO), respectively. Compared with graphite, GO and RGO-CTSO displayed a more intense D band, which resulted from the decrease in the size of the in-plane sp^2 domains during chemical preparation.[31−36] The intensity ratio of the D and G bands of RGO-CTSO (1.06) was lower than that of RGO synthesized by direct chemical reduction of GO, which indicated that functionalization of CTSO on the surface of GO was helpful for chemical preparation of RGO with fewer defects.[37]

The colloidal stability of RGO-CTSO in the water was revealed by its ζ potential. As shown in Figure 3B, the ζ potential of RGO-CTSO was largely dependent on pH. When the pH was <5.3, the ζ potential of RGO-CTSO was >30 mV. When the pH was adjusted to 7.4, the ζ potential of RGO-CTSO reached −27 mV because of the residual carboxyl on the RGO. The ζ potential value well indicates the stability of the colloidal solution. The absolute value of the ζ potential is >30 mV, which generally means enough mutual repulsion to stabilize the colloidal solution.[26] The RGO-CTSO colloidal solution (0.1 mg mL^{-1}) could be stable at pH 2.85 for more than one month, but unstable in an alkaline solution (pH >8.0) after a long period of time because the hydrogen bonding and electrostatic interaction between CTSO and RGO were slowly destroyed.

Because it is positively charged and highly dispersed in the acidic solution, RGO-CTSO as an electrode material for MFCs is expected to increase the contacting surface area, which consequently promotes the electron transfer between the modified electrode and microbial surface. Electron transfer behaviors of *E. coli* on GCE modified with RGO or RGO-CTSO were investigated. CV at 100 mV s^{-1} in Figure 4A showed two pairs of well-defined redox peaks at −0.564 and −0.482 V (termed peak 1) and −0.418 and −0.357 V (termed peak 2) on RGO-CTSO-modified GCE in a PBS solution, suggesting that *E. coli* was electrochemically active on RGO-CTSO-modified GCE.[10,38] However, there was only one pair of weak redox peaks at −0.564 and −0.482 V on RGO-modified GCE, and no redox peak was observed on GCE, which indicated that *E. coli* could not directly interact with GCE or RGO-modified GCE.[1] CV curves of *E. coli* on RGO-CTSO-modified GCE with different scan rates were recorded, as shown in Figure 4B. The anodic peak current (peak 1) was proportional to the square root of the scan rate (Figure 4C), indicating that the electrochemical process for peak 1 is diffusion-controlled.[1] The anodic peak current (peak 2) displayed a linear relation versus the scan rate (Figure 4D), indicating that the electrochemical process for peak 2 was controlled by the surface reaction.[1] The electrochemical reaction for peak 1 was likely due to DET from the cell-excreted accumulated mediators.[4] The reaction for peak 2 might result from redox species on the surface of *E. coli*, which allowed DET of *E. coli* on RGO-CTSO-modified GCE.[1,38] Adhesion and growth ought to be largely restrained because of the repulsion of the negative charge of *E. coli* and RGO, which

DOI: 10.1021/acsami.5b00297
ACS Appl. Mater. Interfaces 2015, 7, 8539−8544

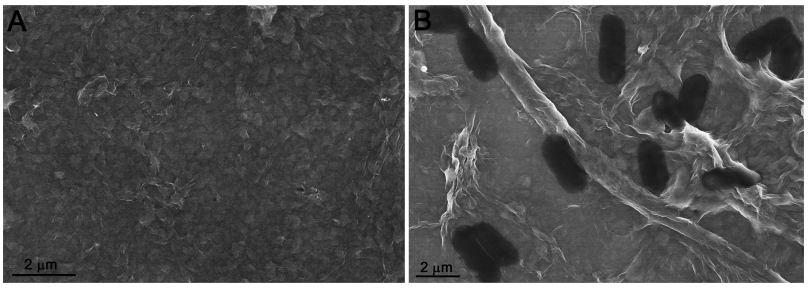

Figure 5. SEM images of (A) RGO or (B) RGO-CTSO film on silicon substrate after immersion in 5 mL of LB liquid culture medium containing *E. coli* for 12 h.

led to an ineffective DET between redox species on the surface of *E. coli* and RGO-modified GCE. CTSO on RGO nanosheets was electropositive and could provide the sites for adhesion growth of *E. coli*, which induced effective DET between redox species of *E. coli* and RGO-CTSO-modified GCE. The interaction of *E. coli* with RGO or RGO-CTSO was further confirmed by SEM characterization. There were a large number of *E. coli* adhering to and growing on the surface of the silicon substrate coated with RGO-CTSO (Si/RGO-CTSO) after Si/RGO-CTSO had been incubated in 5 mL of LB liquid culture medium containing *E. coli* for 12 h (Figure 5B). Nevertheless, no *E. coli* was observed on the surface of the silicon substrate coated with RGO (Figure 5A). Therefore, RGO-CTSO displayed a greater affinity for adhesion growth of *E. coli* in contrast to that of RGO and was superior as an anode material in MFCs.

4. CONCLUSIONS

In summary, highly water-dispersed RGO-CTSO was synthesized by a colloidal chemistry method with biocompatible and water-soluble CTSO as a stabilizer during reduction. The prepared RGO-CTSO showed good colloidal stability in an acidic solution. *E. coli* could adhere to and grow on RGO-CTSO-modified GCE, demonstrating evident electrochemical activity for DET. Compared with RGO, RGO-CTSO provided more activation centers for the adhesion growth of *E. coli* and thus promoted its DET on the modified electrode. The enhanced DET performance of RGO-CTSO made it promising as an anode material of MFCs with *E. coli* as a biocatalyst.

AUTHOR INFORMATION

Corresponding Authors

*E-mail: iamlhwang@njupt.edu.cn.
*E-mail: lxweng@njupt.edu.cn.
*E-mail: wei-huang@njut.edu.cn.

Author Contributions

Z.L. and D.Y. contributed equally to this work.

Notes

The authors declare no competing financial interest.

ACKNOWLEDGMENTS

This work was supported by the National Basic Research Program of China (2012CB933301), the National Natural Science Foundation of China (81273409), the Ministry of Education of China (IRT1148, 20123223110007), the Priority Academic Program Development of Jiangsu Higher Education Institutions (PAPD), and the China Postdoctoral Science Foundation (2013M541700).

ABBREVIATIONS

GO, graphene oxide; RGO, reduced graphene oxide; CTSO, chitosan oligosaccharide; GCE, glassy carbon electrode

REFERENCES

(1) Liu, J.; Qiao, Y.; Guo, C. X.; Lim, S.; Song, H.; Li, C. M. Graphene/Carbon Cloth Anode for High-Performance Mediatorless Microbial Fuel Cells. *Bioresour. Technol.* **2012**, *114*, 275−280.
(2) Logan, B. E. Exoelectrogenic Bacteria That Power Microbial Fuel Cells. *Nat. Rev. Microbiol.* **2009**, *7*, 375−381.
(3) Mohan, S. V.; Chandrasekhar, K. Solid Phase Microbial Fuel Cell (SMFC) for Harnessing Bioelectricity from Composite Food Waste Fermentation: Influence of Electrode Assembly and Buffering Capacity. *Bioresour. Technol.* **2011**, *102*, 7077−7085.
(4) Qiao, Y.; Li, C. M.; Bao, S.-J.; Lu, Z.; Hong, Y. Direct Electrochemistry and Electrocatalytic Mechanism of Evolved *Escherichia coli* Cells in Microbial Fuel Cells. *Chem. Commun.* **2008**, *11*, 1290−1292.
(5) Park, D. H.; Zeikus, J. G. Improved Fuel Cell and Electrode Designs for Producing Electricity from Microbial Degradation. *Biotechnol. Bioeng.* **2003**, *81*, 348−355.
(6) Watanabe, K. Recent Developments in Microbial Fuel Cell Technologies for Sustainable Bioenergy. *J. Biosci. Bioeng.* **2008**, *106*, 528−536.
(7) Geim, A. K.; Novoselov, K. S. The Rise of Graphene. *Nat. Mater.* **2007**, *6*, 183−191.
(8) Huang, X.; Qi, X.; Boey, F.; Zhang, H. Graphene-Based Composites. *Chem. Soc. Rev.* **2012**, *41*, 666−686.
(9) Stankovich, S.; Dikin, D. A.; Dommett, G. H.; Kohlhaas, K. M.; Zimney, E. J.; Stach, E. A.; Piner, R. D.; Nguyen, S. T.; Ruoff, R. S. Graphene-Based Composite Materials. *Nature* **2006**, *442*, 282−286.
(10) Zhang, T.; Cui, C.; Chen, S.; Ai, X.; Yang, H.; Shen, P.; Peng, Z. A Novel Mediatorless Microbial Fuel Cell Based on Direct Biocatalysis of *Escherichia coli*. *Chem. Commun.* **2006**, *21*, 2257−2259.
(11) Cho, J.; Grant, J.; Piquette-Miller, M.; Allen, C. Synthesis and Physicochemical and Dynamic Mechanical Properties of a Water-Soluble Chitosan Derivative as a Biomaterial. *Biomacromolecules* **2006**, *7*, 2845−2855.
(12) Hu, Y.; Jiang, X.; Ding, Y.; Ge, H.; Yuan, Y.; Yang, C. Synthesis and Characterization of Chitosan−Poly (acrylic acid) Nanoparticles. *Biomaterials* **2002**, *23*, 3193−3201.
(13) Wang, S.; Shen, L.; Zhang, W.; Tong, Y. Preparation and Mechanical Properties of Chitosan/Carbon Nanotubes Composites. *Biomacromolecules* **2005**, *6*, 3067−3072.
(14) Hummers, W. S., Jr.; Offeman, R. E. Preparation of Graphitic Oxide. *J. Am. Chem. Soc.* **1958**, *80*, 1339.
(15) Luo, Z.; Yuwen, L.; Han, Y.; Tian, J.; Zhu, X.; Weng, L.; Wang, L. Reduced Graphene Oxide/PAMAM-Silver Nanoparticles Nanocomposite Modified Electrode for Direct Electrochemistry of Glucose Oxidase and Glucose Sensing. *Biosens. Bioelectron.* **2012**, *36*, 179−185.
(16) Han, Y.; Luo, Z.; Yuwen, L.; Tian, J.; Zhu, X.; Wang, L. Synthesis of Silver Nanoparticles on Reduced Graphene Oxide under Microwave Irradiation with Starch as an Ideal Reductant and Stabilizer. *Appl. Surf. Sci.* **2013**, *266*, 188−193.

DOI: 10.1021/acsami.5b00297
ACS Appl. Mater. Interfaces 2015, 7, 8539−8544

(17) Luo, Z.; Yuwen, L.; Bao, B.; Tian, J.; Zhu, X.; Weng, L.; Wang, L. One-Pot, Low-Temperature Synthesis of Branched Platinum Nanowires/Reduced Graphene Oxide (BPtNW/RGO) Hybrids for Fuel Cells. *J. Mater. Chem.* **2012**, *22*, 7791−7796.
(18) Park, S.; Dikin, D. A.; Nguyen, S. T.; Ruoff, R. S. Graphene Oxide Sheets Chemically Cross-linked by Polyallylamine. *J. Phys. Chem. C* **2009**, *113*, 15801−15804.
(19) He, H.; Klinowski, J.; Forster, M.; Lerf, A. A New Structural Model for Graphite Oxide. *Chem. Phys. Lett.* **1998**, *287*, 53−56.
(20) He, H.; Riedl, T.; Lerf, A.; Klinowski, J. Solid-State NMR Studies of the Structure of Graphite Oxide. *J. Phys. Chem.* **1996**, *100*, 19954−19958.
(21) Stankovich, S.; Piner, R. D.; Chen, X.; Wu, N.; Nguyen, S. T.; Ruoff, R. S. Stable Aqueous Dispersions of Graphitic Nanoplatelets Via the Reduction of Exfoliated Graphite Oxide in the Presence of Poly(sodium 4-styrenesulfonate). *J. Mater. Chem.* **2006**, *16*, 155−158.
(22) Lerf, A.; He, H.; Forster, M.; Klinowski, J. Structure of Graphite Oxide Revisited. *J. Phys. Chem. B* **1998**, *102*, 4477−4482.
(23) Stankovich, S.; Piner, R. D.; Nguyen, S. T.; Ruoff, R. S. Synthesis and Exfoliation of Isocyanate-Treated Graphene Oxide Nanoplatelets. *Carbon* **2006**, *44*, 3342−3347.
(24) Cai, W.; Piner, R. D.; Stadermann, F. J.; Park, S.; Shaibat, M. A.; Ishii, Y.; Yang, D.; Velamakanni, A.; An, S. J.; Stoller, M. Synthesis and Solid-State NMR Structural Characterization of ^{13}C-Labeled Graphite Oxide. *Science* **2008**, *321*, 1815−1817.
(25) Yang, X.; Tu, Y.; Li, L.; Shang, S.; Tao, X. Well-Dispersed Chitosan/Graphene Oxide Nanocomposites. *ACS Appl. Mater. Interfaces* **2010**, *6*, 1707−1713.
(26) Villar-Rodil, S.; Paredes, J. I.; Martínez-Alonso, A.; Tascón, J. M. Preparation of Graphene Dispersions and Graphene-Polymer Composites in Organic Media. *J. Mater. Chem.* **2009**, *19*, 3591−3593.
(27) Li, D.; Müller, M. B.; Gilje, S.; Kaner, R. B.; Wallace, G. G. Processable Aqueous Dispersions of Graphene Nanosheets. *Nat. Nanotechnol.* **2008**, *3*, 101−105.
(28) Kolhe, P.; Kannan, R. M. Improvement in Ductility of Chitosan through Blending and Copolymerization with PEG: FTIR Investigation of Molecular Interactions. *Biomacromolecules* **2003**, *4*, 173−180.
(29) Yang, Q.; Pan, X.; Huang, F.; Li, K. Fabrication of High-Concentration and Stable Aqueous Suspensions of Graphene Nanosheets by Noncovalent Functionalization with Lignin and Cellulose Derivatives. *J. Phys. Chem. C* **2010**, *114*, 3811−3816.
(30) Park, S.; Ruoff, R. S. Chemical Methods for the Production of Graphenes. *Nat. Nanotechnol.* **2009**, *4*, 217−224.
(31) Ferrari, A.; Meyer, J.; Scardaci, V.; Casiraghi, C.; Lazzeri, M.; Mauri, F.; Piscanec, S.; Jiang, D.; Novoselov, K.; Roth, S. Raman Spectrum of Graphene and Graphene Layers. *Phys. Rev. Lett.* **2006**, *97*, 187401−187404.
(32) Ferrari, A.; Robertson, J. Interpretation of Raman Spectra of Disordered and Amorphous Carbon. *Phys. Rev. B* **2000**, *61*, 14095−14107.
(33) Schönfelder, R.; Rümmeli, M.; Gruner, W.; Löffler, M.; Acker, J.; Hoffmann, V.; Gemming, T.; Büchner, B.; Pichler, T. Purification-Induced Sidewall Functionalization of Magnetically Pure Single-Walled Carbon Nanotubes. *Nanotechnology* **2007**, *18*, 375601.
(34) Tuinstra, F.; Koenig, J. L. Raman Spectrum of Graphite. *J. Chem. Phys.* **1970**, *53*, 1126.
(35) Wang, Y.; Ni, Z.; Yu, T.; Shen, Z.; Wang, H.; Wu, Y.; Chen, W.; Shen Wee, A. T. Raman Studies of Monolayer Graphene: The Substrate Effect. *J. Phys. Chem. C* **2008**, *112*, 10637−10640.
(36) Yu, Q.; Jauregui, L. A.; Wu, W.; Colby, R.; Tian, J.; Su, Z.; Cao, H.; Liu, Z.; Pandey, D.; Wei, D. Control and Characterization of Individual Grains and Grain Boundaries in Graphene Grown by Chemical Vapour Deposition. *Nat. Mater.* **2011**, *10*, 443−449.
(37) Zhou, Y.; Bao, Q.; Tang, L. A. L.; Zhong, Y.; Loh, K. P. Hydrothermal Dehydration for the "Green" Reduction of Exfoliated Graphene Oxide to Graphene and Demonstration of Tunable Optical Limiting Properties. *Chem. Mater.* **2009**, *21*, 2950−2956.
(38) Zhang, T.; Cui, C.; Chen, S.; Yang, H.; Shen, P. The Direct Electrocatalysis of *Escherichia coli* through Electroactivated Excretion in Microbial Fuel Cell. *Electrochem. Commun.* **2008**, *10*, 293−297.

DOI: 10.1021/acsami.5b00297
ACS Appl. Mater. Interfaces 2015, 7, 8539−8544